05

Multi-frequency generation in Josephson junction arrays

© M.A. Galin[1], L.S. Revin[1,2], M.Yu. Levichev[1], A.E. Parafin[1], D.V. Masterov[1], V.V. Kurin[1], I.A. Shereshevsky[1], N.K. Vdovicheva[1]

[1] Institute for Physics of Microstructures, Russian Academy of Sciences, Nizhny Novgorod, Russia
[2] Nizhny Novgorod State Technical University n. a. R.E. Alekseev, Nizhny Novgorod, Russia
E-mail: galin@ipmras.ru

Received April 14, 2025
Revised June 11, 2025
Accepted June 11, 2025

The phenomenon of multi-frequency generation was revealed in experimental study of electromagnetic radiation spectra of a large low-temperature Josephson junction array fabricated on the basis of niobium. The array spectrum was measured by a superconducting receiver with a high-temperature bicrystal Josephson junction. Numerical simulation of Josephson system similar to that studied experimentally showed that the multi-frequency generation regime occurs when the junction array contains eigenmodes with close frequencies.

Keywords: Josephson junction array, bicrystal Josephson junction, spectroscopy, FDTD method, resonator.

DOI: 10.61011/TPL.2025.09.61817.20344

Nonlinear properties of the Josephson junction manifest themselves, for instance, in the ac voltage generation when the applied direct current exceeds the critical one. Thereat, the junction emits an electromagnetic signal in the millimeter or terahertz range. However, power of this signal is very low and doesn't exceed the picowatt level [1,2]. Detected power is further suppressed because of a significant mismatch of junction with the external environment, dissipation of radiation in the surrounding structure, and large fraction of higher harmonics in the spectrum [2].

To achieve the generation power sufficient for practical applications, it is necessary to use arrays of Josephson junctions. Typically, the arrays consist of lumped junctions whose size l does not exceed Josephson penetration depth λ_J. Contrary to a long Josephson junction with $l \gg \lambda_J$, the lumped junction array does not need a control line to induce magnetic field; synchronization of junctions potentially allows achieving a narrow generation line whose width is inversely proportional to the number of synchronized junctions [3].

This paper is devoted to spectral studies of an array of low-temperature junctions fabricated on the basis of niobium. Such arrays are in demand as voltage standards; their manufacturing technique is being permanently improved. They are characterized by a small spread of critical currents of Josephson junctions ($\sim 2-3\,\%$) [4], which allows producing programmable circuits of voltage standards containing $\sim 10^5$ junctions [5]. In this respect, Josephson junctions of other types cannot compete with them: high-temperature junctions have much worse reproducibility [6,7], while internal junctions based on the BiSrCaCuO compound have an additional problem, that is, nonuniform heating [8,9]. Small spread of parameters, jointly with a favorable topology of the superconducting circuit and large number of junctions, gives hope for obtaining a sufficiently narrow spectral line of Josephson generation. The initially narrow line of generation makes simpler the procedure of the phase-locked loop frequency control which additionally narrows the line to the extent necessary for practical applications, for instance, for using the array as a local oscillator [10,11]. This study revealed the effect of the array generation at several frequencies simultaneously. In the above-mentioned applications of the junction array, this effect is parasitic, but may appear to be useful in other research and technological tasks.

The investigated array contains 9996 Nb/NbSi/Nb Josephson junctions grown on a silicon substrate (Fig. 1). The junctions are distributed among seven identical sections. Each section consists of three single-strip lines (SSLs) 7.1 mm long; each SSL contains 476 junctions. Geometrically, SSLs are parallel to each other and connected in series by direct current. Between the sections there are contact pads that allow connecting to the power source either the entire array or its individual parts. The junction size is $8 \times 8\,\mu$m, the thickness of NbSi interlayer is about 10 nm. Procedure for fabricating such junctions is described in [4,12].

The array's I-V characteristic is shown in Fig. 2. The hysteresis occurs due to non-simultaneous transitions of individual junctions from the resistive state to superconducting one [13]. The resistive branch of the array's I-V curve consists of separate sections of higher differential conductivity or steps also separated from each other by hysteresis transitions. Those steps stem from resonances arising in the array when the Josephson junction frequencies coincide with the leaky mode ones. The resonances are excited in the array's straight parts (SSLs) that constitute each section. Study [11] has shown for a similar array that the length of such SSLs corresponds to the average interstep distance Δf_J represented in the values of Josephson frequency f_J averaged over all junctions in the array if each

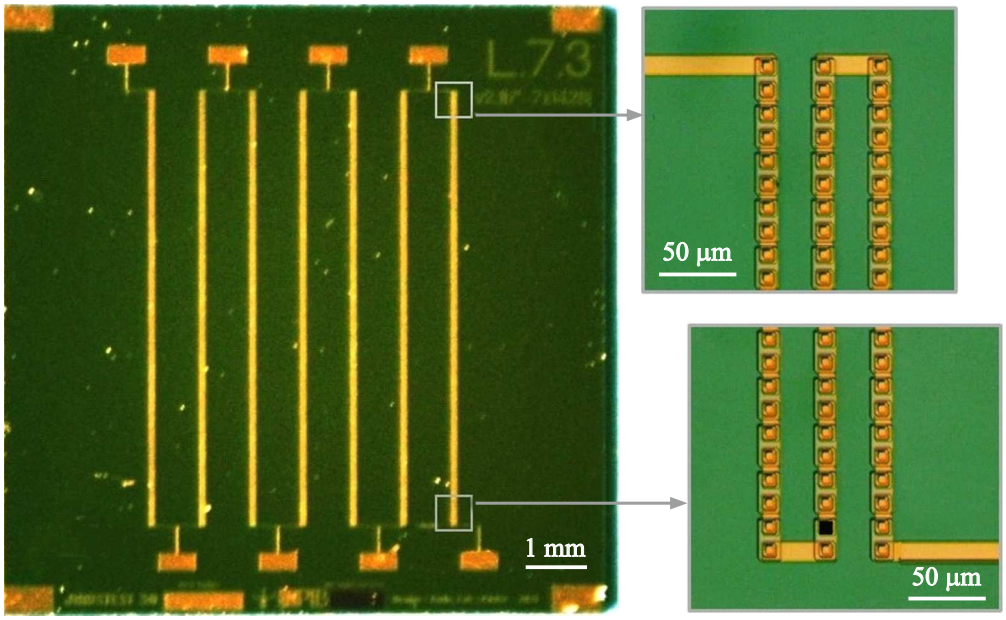

Figure 1. A photograph of the Nb/NbSi/Nb Josephson junction array. The insets present the array fragments. The black square in the lower inset shows the position of one of the junctions.

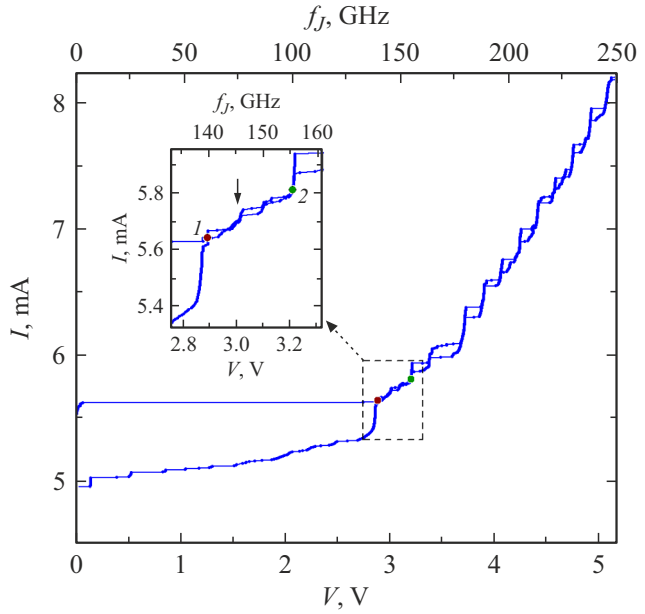

Figure 2. I-V characteristic of the Josephson junction array. The upper axis plots the Josephson frequency averaged over the entire array. The measurements presented in Fig. 3 were performed at the points marked in the inset. The arrow indicates the step to which the second spectral line (Fig. 3, *a*) corresponds.

SSL is regarded as a single-strip resonator located at the substrate-air interface. For the array investigated in this paper we have $\Delta f_J = 8.2\,\text{GHz}$ which is lower than that for the array studied in [11] because of a larger SSL length: 7.1 mm instead of 5 mm.

Nevertheless, no ideal equidistance between the steps is observed. In addition, the I-V curve exhibits a finer structure in the form of smaller steps, smooth transitions between the steps, etc. This may be explained by a more complex structure of resonant system in the array, that cannot be reduced to a one-dimensional resonator in the form of SSL. This is shown in [14] where the array was scanned by a low-temperature laser microscope, which allowed visualization of distribution of the electromagnetic field excited in the array. The results of [14] revealed a strong coupling between SSLs constituting one section, that actually leads to formation of a two-dimensional mode structure throughout the entire section. In addition, paper [15] has shown that the substrate can also participate in formation of modes.

The sample was cooled with liquid helium in a dewar. Josephson radiation was coupled out through a waveguide path. As in [16], the measurements were performed with a receiver whose mixer was a high-temperature Josephson junction formed on the bicrystal boundary of an yttria-stabilized zirconia substrate. In [16], the spectrum for both the entire array and its part always exhibited a single line corresponding to a certain resonance. The line width varied from 0.3 to $\sim 10\,\text{MHz}$ depending on the power supply type and technical noise level. It was noted that at the edges of the main I-V curve steps, as well as at small steps, the spectrum line positions may differ significantly from f_J. It was suggested that such a strong frequency shift is associated with simultaneous excitation in the array of two resonances corresponding to neighboring I-V curve steps. Measurements presented in this paper have confirmed this hypothesis.

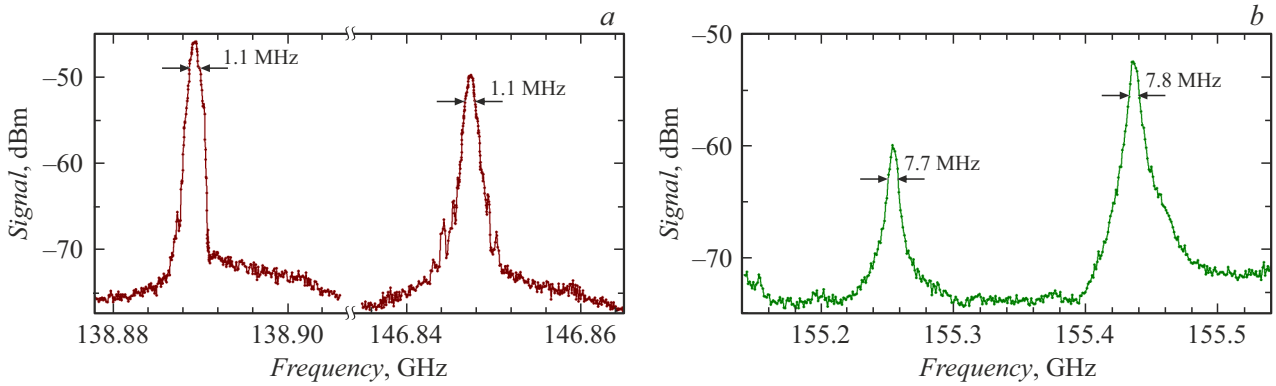

Figure 3. The Josephson generation spectrum measured at the I-V curve points *1* (*a*) and *2* (*b*) marked in Fig. 2. For each line, its width measured at the level of 1/2 of the maximum is indicated.

Fig. 3, *a* shows the generation spectrum measured by moving along the I-V curve to the upper edge of the first step (point *1* in the Fig. 2 inset). Power was supplied by current source Keithley 6221. The measurements cover the frequency range of 8 GHz at the edges of which two spectral lines ~ 1 MHz wide are observed. They cannot be observed simultaneously because of the limited bandwidth of the intermediate frequency amplifiers (~ 2 GHz); therefore, to make possible detecting the second line, the local oscillator frequency was varied at the fixed position of operating point. The left spectral line is associated with the resonance excitation at the I-V curve step where the operating point is located. This step is located in the range $f_J = 138-139$ GHz, which agrees with the position of the line in the spectrum. The right line is most likely associated with the resonance excitation on one of two small steps located between two main steps. This step is indicated by the arrow in the inset to Fig. 2. It belongs to range $f_J = 145-146$ GHz, which approximately corresponds to the position of the right line in the spectrum. A slight difference between this position and f_J may be explained by the contribution to f_J from the asynchronous array junctions [17].

Fig. 3, *b* presents the spectrum of the array measured at the lower edge of the second main step of the I-V curve (point *2* in the Fig. 2 inset). The spectrum contains two lines of Josephson generation about 8 MHz wide. They are separated from each other by less than 200 MHz, due to which the superconducting receiver is able to detect them simultaneously. Frequencies of these lines correspond well to the position of operating point at the I-V curve. Despite the lines are considerably wider and lower than those shown in Fig. 3, *a*, they are of the same nature, i. e., they are lines of the two-frequency resonance excitation corresponding to the second main step. Thus, resonant modes may get split even within one step because of complexity of the system structure into which the Josephson junction array is embedded.

Experimentally observed two-frequency generation of the Josephson junction array was confirmed by the results of numerical simulation. The computational algorithm combines the Finite Difference Time Domain (FDTD) method with equations of the resistive junction model [18]. The radiating system named Josephson antenna includes an arbitrary number of junctions, EMF sources, and linear passive elements which are connected by thin ideal wires into a single circuit. The antenna may be placed on a substrate. A more detailed description of the calculation method may be found in [17] together with the results of calculations of the I-V characteristics, radiated power, ac current and voltage spectra, and radiation pattern [17].

The simulated Josephson antenna consists of seven lines $L = 1.8$ mm long connected in parallel to each other (Fig. 4, *a*). In the central line there is mounted the EMF source with internal resistance of 50 Ω, while other lines contain 40 Josephson junctions each. The critical current, normal resistance and McCumber parameter of junction are $I_c = 2.5$ mA, $R_n = 0.5\,\Omega$ and $\beta = 0.2$, respectively. At the end of each line with junctions, an inductance is also located. These inductances for two lines that are second from the upper and lower antenna edges are 0.1 nH, those for the rest lines are 0.4 nH. Inductances of 0.1 nH are also located on the left in the short vertical segments connecting each line. They are designed for ac decoupling of the line with the EMF source and lines with junctions. The substrate is not used; the surrounding space is vacuum.

Fig. 4, *b* presents I-V characteristic of the second antenna line recorded with increasing EMF from 700 to 945 mV. As in the measurements (Fig. 2), the I-V characteristic exhibits inclined steps arising due to the resonance excitation in the line with junctions. Transitions between the steps, as well as transition to the resistive branch of I-V curve, are inclined negatively because of the finite source resistance.

Fig. 4, *c* shows the result of calculation the ac spectrum amplitude in the line under consideration at the bias current of 2.7 mA which corresponds to the position between the second and third I-V curve steps (Fig. 4, *b*). The spectrum exhibits three resonant modes which are standing waves with different numbers of antinodes: the lower mode has three antinodes, two upper modes have

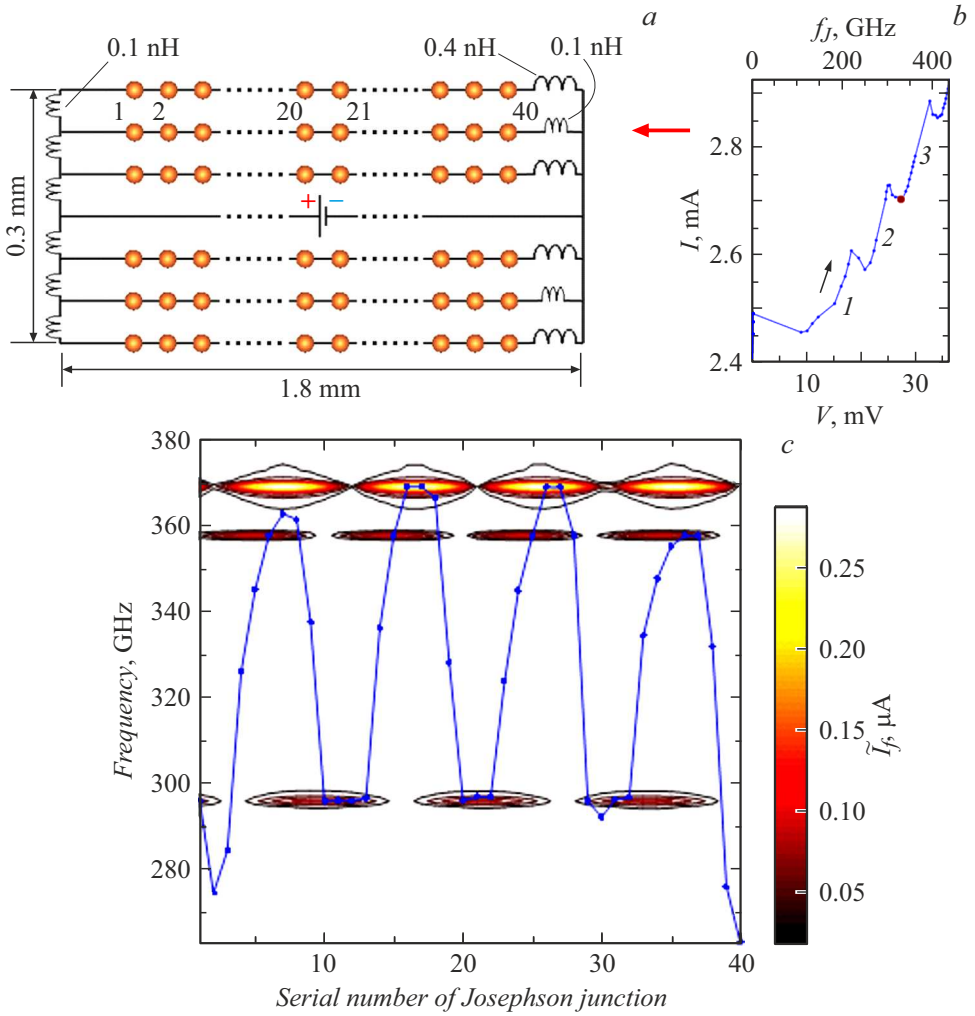

Figure 4. *a* — The circuit of Josephson antenna selected for numerical simulation. Circles represent the Josephson junctions, some of which are numbered. The antenna's inductances, length and width are also indicated. The power supply is depicted in the center. *b* — I-V characteristic of the second line of Josephson antenna. The upper axis plots the Josephson frequency averaged over the junctions in the line. The arrow indicates the direction of recording of the I-V curve. Digits *1–3* designate the steps. The ac spectrum was calculated at the point indicated in the I-V curve. *c* — spectrum of ac current amplitude versus the number of junction in the second line. The solid line superimposed on the spectrum indicates the distribution of Josephson frequency over the junctions.

four ones. The number of antinodes determines the resonance number with which a certain I-V curve step is typically associated. The frequency of lower mode is $f = 296\,\text{GHz}$, which corresponds to the upper edge of the second step, while frequencies of upper modes are $f \approx 360{-}370\,\text{GHz}$, which corresponds to the center of the third step (Fig. 4, *b*). Note also that the lower mode is approximately $60{-}70\,\text{GHz}$ apart the upper ones; this value agrees well with fundamental frequency f_0 of a thin antenna L long: $f_0 = c/(2L) = 83.3\,\text{GHz}$, where $c = 3 \cdot 10^{11}$ mm/s is the speed of light in vacuum. All of the above allows us to assert that the lower mode corresponds to the second step, while the upper modes correspond to the third step. The simulation results are similar to the spectra obtained in measurements on the niobium junction array, where both relatively distant lines corresponding to adjacent I-V curve steps (Fig. 3, *a*) and close lines belonging to one and the same step (Fig. 3, *b*) were also observed.

Generation of two close spectral lines corresponding to one and the same step of I-V characteristic is explained by elimination of the eigenmodes degeneracy of the resonant system due to the coupling between lines with junctions. The degeneracy gets eliminated due to the difference in inductances of adjacent lines which leads to a difference of their electrical lengths, and, hence, a difference of partial frequencies from similar quantities for the entire resonant system. Thus, we can state that one of the upper modes shown in Fig. 4, *c* is determined by the partial mode of the second line, while the other one is determined by partial modes of neighboring lines. Due to the interaction of lines with each other, natural frequencies get shifted with respect to partial ones. This may explain the shift in the position

of the lower mode (Fig. 4, *c*) relative to the center of the second step of I-V curve.

Thus, both measurements and numerical simulation have revealed the possibility of generation of the Josephson junction array at several frequencies. Obviously, the revealed effect prevents efficient application of junction array as a local oscillator for conventional superheterodyne receivers. The effect of multi-frequency generation may be neutralized by increasing the quality factor of resonators, which are here the sections of SSL. It is also necessary to minimize electromagnetic rereflections occurring at the bends and at the transitions to the contact pads, since those rereflections give rise to secondary resonances at close frequencies. On the other hand, multi-frequency generation may be useful in a number of applications: in multiband radar systems for generating multi-frequency phase-coded signals [19], in microwave interferometry for monitoring plasma characteristics in tokamaks [20], etc. Under certain conditions, the Josephson junction array may prove to be a good alternative to conventional oscillators used in such applications; thus, a need to evolve the revealed multi-frequency generation effect may arise.

Funding

The study was supported by the Russian Science Foundation (project No 20-79-10384-P).

Conflict of interests

The authors declare that they have no conflict of interests.

References

[1] I.K. Yanson, V.M. Svistunov, I.M. Dmitrenko, JETP, **21** (3), 650 (1965).
[2] M. Darula, T. Doderer, S. Beuven, Supercond. Sci. Technol., **12** (1), R1 (1999). DOI: 10.1088/0953-2048/12/1/001
[3] A.K. Jain, K.K. Likharev, J.E. Lukens, J.E. Sauvageau, Phys. Rep., **109**, 309 (1984). DOI: 10.1016/0370-1573(84)90002-4
[4] O. Kieler, R. Wendisch, R.-W. Gerdau, T. Weimann, J. Kohlmann, R. Behr, IEEE Trans. Appl. Supercond., **31** (5), 1100705 (2021). DOI: 10.1109/TASC.2021.3060678
[5] S. Bauer, R. Behr, J. Herick, O. Kieler, M. Kraus, H. Tian, Y. Pimsut, L. Palafox, Meas. Sci. Technol., **34** (3), 032001 (2023). DOI: 10.1088/1361-6501/aca5a5
[6] S.K.H. Lam, J. Lazar, J. Du, C.P. Foley, Supercond. Sci. Technol., **27** (5), 055011 (2014). DOI: 10.1088/0953-2048/27/5/055011
[7] K.-H. Müller, E.E. Mitchell, Phys. Rev. B, **109** (5), 054057 (2024). DOI: 10.1103/PhysRevB.109.054507
[8] D. Oikawa, H. Mitarai, H. Tanaka, K. Tsuzuki, Y. Kumagai, T. Sugiura, H. Andoh, T. Tsukamoto, Appl. Phys. Lett., **10** (8), 085113 (2020). DOI: 10.1063/5.0018989
[9] M.M. Krasnov, N.D. Novikova, R. Cattaneo, A.A. Kalenyuk, V.M. Krasnov, Beilstein J. Nanotechnol., **12**, 1392 (2021). DOI: 10.3762/bjnano.12.103
[10] V.P. Koshelets, M. Birk, D. Boersma, J. Dercksen, P.N. Dmitriev, M.I. Faley, L.V. Filippenko, K.V. Kalashnikov, N.V. Kinev, O.S. Kiselev, A.A. Artanov, K.I. Rudakov, A. de Lange, G. de Lange, V.L. Vaks, M.Y. Li, H. Wang, IEEE Trans. Appl. Supercond., **5** (4), 687 (2015). DOI: 10.1109/tthz.2015.2443500
[11] M.A. Galin, A.M. Klushin, V.V. Kurin, S.V. Seliverstov, M.I. Finkel, G.N. Goltsman, F. Müller, T. Scheller, A.D. Semenov, Supercond. Sci. Technol., **28** (5), 055002 (2015). DOI: 10.1088/0953-2048/28/5/055002
[12] F. Mueller, R. Behr, T. Weimann, L. Palafox, D. Olaya, P.D. Dresselhaus, S.P. Benz, IEEE Trans. Appl. Supercond., **19** (3), 981 (2009). DOI: 10.1109/TASC.2009.2017911
[13] M.A. Galin, E.A. Borodianskyi, V.V. Kurin, I.A. Shereshevsky, N.K. Vdovicheva, V.M. Krasnov, A.M. Klushin, Phys. Rev. Appl., **9** (5), 054032 (2018). DOI: 10.1103/PhysRevApplied.9.054032
[14] M.A. Galin, F. Rudau, E.A. Borodianskyi, V.V. Kurin, D. Koelle, R. Kleiner, V.M. Krasnov, A.M. Klushin, Phys. Rev. Appl., **14** (1), 024051 (2020). DOI: 10.1103/PhysRevApplied.14.024051
[15] F. Song, F. Müller, R. Behr, A.M. Klushin, Appl. Phys. Lett., **95** (17), 172501 (2009). DOI: 10.1063/1.3253417
[16] M.A. Galin, L.S. Revin, A.V. Samartsev, M.Yu. Levichev, A.I. El'kina, D.V. Masterov, A.E. Parafin, Tech. Phys., **69** (7), 973 (2024). DOI: 10.61011/TP.2024.07.58800.166-24.
[17] M.A. Galin, I.A. Shereshevsky, N.K. Vdovicheva, V.V. Kurin, Supercond. Sci. Technol., **34** (7), 075005 (2021). DOI: 10.1088/1361-6668/abfd0b
[18] K.K. Likharev, *Dynamics of Josephson Junctions and Circuits* (Gordon and Breach Science Publishers, New York, NY, USA, 1986), pp. 45-47.
[19] Y. Chen, L. Jiang, Q. Liu, IEEE Photon. Technol. Lett., **32** (16), 975 (2020). DOI: 10.1109/LPT.2020.3006881
[20] M. Varavin, A. Varavin, D. Naydenkova, J. Zajac, F. Zacek, S. Nanobashvili, R. Panek, V. Weinzettl, P. Bilkova, K. Kovarik, F. Jaulmes, M. Farnik, M. Imrisek, O. Bogar, Fusion Eng. Des., **146**, 1858 (2019). DOI: 10.1016/j.fusengdes.2019.03.051

Translated by EgoTranslating